CONTROL STRATEGY FOR CURBING VOLTAGE REGULATION ISSUES CAUSED BY INTERMITTENCY OF RES IN A RADIAL MICROGRID

DISSERTATION
SUBMITTED IN PARTIAL FULFILLMENT OF THE REQUIREMENTS
FOR THE AWARD OF THE DEGREE
OF

MASTER OF TECHNOLOGY
In
POWER SYSTEM

Submitted by:

Nishant Bansal
(Roll no. 2K14/PSY/14)

Under the supervision of

Prof. Vishal Verma

DEPARTMENT OF ELECTRICAL ENGINEERING

DELHI TECHNOLOGICAL UNIVERSITY

(Formerly Delhi College of Engineering)

Bawana Road, Delhi-110042

2018

DECLARATION

I, NISHANT BANSAL (2K14/PSY/14) hereby declare that the work, which is being presented in the report entitled, **"CONTROL STRATEGY FOR CURBING VOLTAGE REGULATION ISSUES CAUSED BY INTERMITTENCY OF RESs IN A RADIAL MICROGRID"** submitted for partial fulfillment of the requirements for the award of the degree of Master of Technology (Power System) is an authentic record of my own work carried out under the guidance of Dr. VISHAL VERMA, Professor, EED, DTU. The matter embodied in the dissertation work has not been plagiarized from anywhere and the same has not been submitted for the award of any other degree or diploma in full or in part.

Submitted by:-

NISHANT BANSAL
(2K14/PSY/14)
Power System
Electrical Engineering Department

DEPARTMENT OF ELECTRICAL ENGINEERING

DELHI TECHNOLOGICAL UNIVERSITY

(Formerly Delhi College of Engineering)

CERTIFICATE

This is to certify that the thesis entitled, "**CONTROL STRATEGY FOR CURBING VOLTAGE REGULATION ISSUES CAUSED BY INTERMITTENCY OF RESs IN A RADIAL MICROGRID**", submitted by Mr. **NISHANT BANSAL**, Roll No. 2K14/PSY/14, student of Master of Technology (Power System) in Electrical Engineering department from Delhi Technological University (Formerly Delhi College of Engineering), is a dissertation work carried out by him under my guidance during session 2014-2016 towards the partial fulfillment of the requirements for the award of degree of Master of Technology in Power System.

The uniqueness of the thesis pertains to the development of control algorithm for curbing the voltage regulation issues caused by the intermittency of RES in a radial AC microgrid.

I wish him all the best in his endeavors.

(Prof. VISHAL VERMA)

Professor, EED, DTU

ACKNOWLEDGMENT

It is my pleasure to be indebted to various people, who directly and in directly or indirectly contributed in the development of this work and who influenced my thinking, behavior, and during the course of study. Firstly I would like to express my deep sense of gratitude to my respected and learned guide and mentor **Prof. Vishal Verma** (Professor, Electrical Department, DTU) for his guidance and constant supervision as well as for providing necessary information regarding the project & also for his support in completing the project.

I am grateful to **Prof. Madhusudan Singh**, HOD Electrical Department, for his support and acknowledgement.

I would like to extend my thanks to the **Dr. Amritesh Kumar** for his help in completing this thesis.

I would like to express my thanks to PhD Scholars, **Mr. Aditya Narula, Ms. Vandana Arora, Mr. Ramesh Singh, Ms. Ritika Gour, Mr. Shirish Raizada and Ms. Pankhuri Asthana for** their help and supports in making me understand the concept. I also want to thank Mr. Tarun Jangid for his unconditional support and motivation during this work.

Last but not the least; I would like to thank my family for their moral support throughout.

NISHANT BANSAL

2K14/PSY/14

ABSTRACT

With the development in power electronics technology, distributed energy generation using renewable sources of energy such as PV, wind turbines etc. are gaining importance in recent times. Generation of electricity using renewable energy sources can yield power in KW scale or in MW scale. Energy generated using RESs is used to supply power to localized loads at the distribution level. This helps relieve burden on conventional power plants and thus improve reliability of the utility system. With the increase in penetration of distributed generation in recent times it led to the development of microgrids which consist of low voltage distribution systems having distributed energy sources alongwith storage devices. Due to intermittent behaviour of DGs using RESs, it becomes a challenging task to integrate them with the utility grid.

Different types of microgrids such as AC microgrids and DC microgrids operating in various modes such as islanded mode and grid – connected mode have been discussed in detail. Due to the operation of microgrids in islanded mode and grid – connected mode, power electronic engineers face various technical challenges; low inertia of interfacing inverters, power quality related problems, design of protection devices being the most prominent ones have been discussed in detail.

This work gives a detailed description of the mathematical tools and techniques used for the development of control algorithm for current-controlled Battery Energy Storage System (BESS) connected in shunt with the load. Control algorithm is developed for curbing voltage regulation issues caused due to intermittency of RES in a radial microgrid. Conventional droop control is explained in detail and is being implemented in the control algorithm for the creation of virtual inertia following a specific droop rate. MATLAB/Simulink model of the proposed system configuration in which BESS is connected in shunt with the load alongwith RES based DG is discussed in detail. Simulation results of the proposed radial microgrid operating in grid – connected mode for various types of loads are analyzed and are presented in this work.

TABLE OF CONTENTS

LIST OF FIGURES

ABBREVIATIONS

Abbreviations	Full-Form
PV	Photovoltaic
AC	Alternating Current
DC	Direct Current
P&O	Perturb And Observe
InC	Incremental Conductance
CSI	Current Source Inverter
MPPT	Maximum Power Point Tracking
I_{SC}	Short-Circuit Current
V_{OC}	Open-Circuit Voltage
V_{DC}	Dc Link Voltage
VSI	Voltage Source Inverter
DG	Distributed Generation
THD	Total Harmonic Distortion
WT	Wind Turbine
RES	Renewable Energy Source
BESS	Battery Energy Storage System
APF	Active Power Filter
CMC	Current Mode Control
EMI	Electromagnetic Interference
STATCOM	Static Compensator
PWM	Pulse Width Modulation
d-q	Direct-Quadrature
SoC	State Of Charge
EVs	Electric Vehicles
LVRT	Low Voltage Ride Through
BOS	Balance Of System
MATLAB	Matrix Laboratory
PSO	Particle Swam Optimization

HF	High Frequency
VSC	Voltage Source Converter
SPWM	Sinusoidal PWM
BESS	Battery Energy Storage System
CCS	Current Controlled Source
SRF	Synchronous Reference Frame
PLL	Phase Locked Loop
PCC	Point Of Common Coupling
LPF	Low Pass Filter
PI	Proportional Integral
UPF	Unity Power Factor
PQ	Power Quality
HEV	Hybrid Electric Vehicle
PHEV	Plug-In Hybrid Electric Vehicle
LI-ION	Lithium Ion

CHAPTER-1
INTRODUCTION

1.1 GENERAL INTRODUCTION

Majority of the load is being fed by conventional power system having generation of the capacity of GWs using conventional methods which are based on fossil fuels i.e. coal, oil, natural gas etc. The conventional means of generation of electricity i.e. thermal power plants, nuclear power plants, hydroelectric power plants are located at far distances from load centres. With the depletion of natural resources, growing demand, environmental issues and technical issues; lately distributed generation systems using renewable sources of energy such as solar, wind, tidal etc. are being used for the generation of electricity, either at small – scale decentralized systems with capacity in kW scale for supplying power to local loads or even medium – scale systems with capacity in few MW. In contrast to conventional generation system, the distributed generation system involves various generating and storage units; some located close to load centres or even in the vicinity of the loads, reduce burden on the transmission system and further facilitate energy efficiency. Use of renewable sources of energy help improve environmental issues such as reduction in pollution.

Due to intermittent behaviour of renewable energy sources (RES), it posed a big challenge for power engineers to effectively and efficiently utilize renewable energy for power generation. With the advent of power electronics and thus power electronic converters, power conversion from renewable energy sources has become efficient. Among the renewable energy sources, photovoltaic (PV) energy, wind energy and hydropower have largest utilization for distributed RES generation. Due to increase in penetration of distributed generation, its inherent problems are clearly revealed. It poses high installation cost and certain control difficulties [1]. Moreover due to technological advancements in various types of loads like constant power loads, non linear loads, passive loads, critical and non critical loads, it poses the problem of power quality at the load end as well.

With the emergence of new technologies most importantly the development of power electronic interface for integrating multiple DGs of microgrid using appropriate control theory, this concept came into existence. Microgrids are categorized into two types i.e. AC microgrid and DC microgrid. Microgrids operate in either islanded mode or grid-connected mode. In islanded mode, the independent and stable operation of microgrid is supported by distributed energy storage system. In grid – connected mode, microgrid needs some special control modes in order to make it possible to meet the conditions of grid – connected operation. In this thesis control algorithms are developed for the integration of multiple DGs with that of point of common coupling (PCC) of utility grid, for improving power quality of the system. One inherent problem with these RES based DGs is that they are inertia-less because they are being governed through fast control using static switches. To counter such inertia-less DGs developed from RES such as PV, control algorithm is designed to create virtual inertia in the DGs such that stability of the system is maintained regardless of the intermittent behaviour of the DGs.

The following sections and sub-sections give an insight of the art of microgrid, its various modes of operation and issues with integration of multiple RESs in a microgrid. Later brief outline of the scope of work and organization of thesis is presented.

1.2 CONVENTIONAL GENERATION

Due to the excessive increase in demand of electricity, generation of electricity from non – renewable sources of energy like coal, natural gas etc result in depletion of their reserves. This causes an imbalance in the nature which is creating havoc on the earth's ecosystem [2]. Generation from thermal power plants has the largest contribution in electric power generated in India. Thermal power generation in India is about 222.906 GW which contributes to around 58% of the total installed capacity. Thermal power plants emit gases such as CO_2, SO_2 and NO_2 known as greenhouse gases which causes global warming. Cost of fuel, operation and maintenance cost are high. Other problem in thermal power plants is dealing with the waste. Other conventional power plant is nuclear power plant, still the issue of dumping the

radioactive waste is persistent. Hence the shifting towards renewable energy sources for meeting the increased demand is obvious.

1.3 CONCEPT OF DISTRIBUTED GENERATION

Distributed generation refers to the different technologies that generate electricity at the proximity to the load centers thus reducing the burden on the transmission and distribution systems. These technologies can yield power in kW scale or MW scale. Decentralized or distributed generation has various benefits some of which are listed below:

- Reduce peak demand
- Help deal with high peak load shortages problem.
- Improve the grid network reliability by reducing transmission and distribution losses.
- Provide power to remote and inaccessible areas.
- Reduction in land-use effects and right of way acquisition costs.
- Improvement in power quality.

1.3.1 Renewable energy sources (RESs): Basics and issues related to RESs

Renewable energy sources are those which are inexhaustible. Renewable sources of energy include solar power, wind power, hydroelectric power, geothermal power and tidal power. The most important aspect of using renewable sources of energy is that energy can be harnessed without the release of harmful pollutants. Currently the most widely used renewable energy sources for generating electricity are solar energy using PV panels and wind energy using wind turbines.

Currently the most widely used renewable energy sources for generating electricity are solar energy using PV panels and wind energy using wind turbines.

PV system directly converts solar power into electricity using photo-electric effect. These systems are suitable for both on-grid and off-grid operation depending upon the location of load and grid availability. Certain issues related to PV system are high capital cost, generation only during daytime, partial shading effects etc.

Wind turbine converts energy stored in the wind into mechanical energy which can further be converted into electrical energy. Certain issues related to wind energy are the high capital cost investment, design of wind turbines, environmental impact, location issues and grid connection issues etc.

In order to tackle the issues related to renewable energy sources (RESs), efficient means have to be devised for extracting the maximum output power. The development in power electronics has helped the engineers to come up with smaller yet efficient powerful systems to generate electricity from renewable energy sources.

1.3.2 Power Electronic Interface with RES

Power electronics find most important applications in solar and wind energy systems. In the last decade, a constant effort is being put to improve every part of PV and WT application. The efficiency of PV module is about 17%, the efficiency of inverters have almost reached 98-99%. New topologies are developed which make wind turbines operation more efficient.

Systems used in these applications produce DC Current, so inverters are required to convert DC power into AC power so that this power can be utilized in various applications.

1.3.2.1 Power Electronic Interface for PV Applications

Basic parts of PV installation are the PV module, the power electronic devices and circuits and the balance of system (BoS). The PV modules are composed of several solar cells that convert the sunlight energy directly into electricity by photo-electric effect and thus produce desired levels of DC current and voltage.

All PV modules follow a typical current-voltage characteristic curve which are used to make all necessary calculations. The output power of the PV panel is unregulated and in order to get regulated output power DC-DC Converters are used. Different topologies are devised based on the application on the load side. The inverter input scans I-V curve of the string until maximum power point is found thus extracting maximum power through MPPT. In PV applications, VSI are used.

1.3.2.2 PE interface for Wind Turbine Applications

Wind Turbines are categorized into two types: - Horizontal axis and vertical axis; Horizontal axis WT being the most popular design. The wind turbines and the utility grid are connected with each other through power electronics interface thus energy generated by wind turbines feed the produced energy to the utility grid. The frequency of the output power produced from wind turbine varies in accordance to wind speed thus back-to-back converter topologies are used to interface it with the utility grid following the frequency regulations. There are various types of converter topologies that are used in wind turbine installations such as tandem converters, multilevel converters, matrix converters, resonant converters; multilevel converters being the best topology considering the harmonic performance. Apart from the above topologies, what really makes the difference is the control concept. Constant research is being carried out to develop better modulation techniques and to eliminate harmonics in order to minimize the cost of filters.

1.3.3 Issues with PE interface for grid integration of RES

Most widely used Renewable energy sources such as solar photovoltaic and wind energy are intermittent in nature hence it is a challenging task to integrate RES with the utility grid. Various technical issues associated with grid integration of RES are listed below: -

a) Power quality problem due to the use of non-linear power electronic devices.
b) Variability of renewable production due to intermittent nature of RES.
c) Protection issues due to bi-directional flow of power in distribution network.
d) Localized voltage stability problems.
e) Low inertia of power electronic interface converters.

Various techniques and control algorithms have been designed by the researchers to overcome the issues with the grid integration of RES so as to provide reliable and clean energy to localized load centers.

1.4 MICROGRIDS

Microgrids consist of low voltage distribution systems having distributed energy sources together with storage devices and flexible loads.

Different micro-generation systems such as Wind Turbine (WT) or Photo-Voltaic (PV), etc. can directly be connected to LV networks. Such units are located at the distribution side to meet the growing power demand locally thus enhancing reliability and power quality.

Due to increase in the penetration of micro-generation in the LV distribution network; the impact of micro-generation on power balance and grid frequency becomes prominent. Therefore, a control and management architecture is required to facilitate the full integration of micro-generation and active load management into the systems.

1.4.1 AC and DC Microgrids

Microgrids can be identified in following three types based on the currents and voltages adopted in the microgrid: -

1) *AC Microgrid:* In AC Microgrids, all DERs and loads are connected to a common AC bus. RES as well as energy storage units give DC power output which is connected to AC bus via DC-AC inverters.
2) *DC Microgrid:* In DC Microgrids, common bus is DC which is used to supply power to DC loads.
3) *Hybrid Microgrid:* Hybrid Microgrid is a combination of AC and DC Microgrid. This type of microgrid is suitable where both types of buses (i.e. AC as well as DC) exist in order to supply power to both AC and DC loads.

1.4.2 Modes of Operation:

Microgrids may operate in two different modes: -

- Islanded Mode
- Grid-Connected Mode

In islanded mode of operation, microgrid needs to have high storage along with RES in order to satisfy or cater to the load demand. In this mode of operation, when the utility grid is disconnected, DGs continue to provide power through RES with the support of storage devices thus ensuring reliability of the power network. Voltage and frequency of the system are governed by the inverter itself as it is acting as the master in the absence of utility grid i.e. it is operating in voltage control mode.

In grid-connected mode of operation, microgrid supplies or draws power to the utility grid depending on the generation and load demand. The majority of the microgrids operate in grid-connected mode in order to cater to load demand on distribution side, as grid appears an infinite storage. Here the inverter interfaced with RES operates in current control mode.

1.4.3 Technical Challenges on Microgrids

The main function of microgrids is to ensure reliable, stable operation during normal condition and to ensure fast fault clearance without much network disturbances. The increased penetrations of DGs in microgrid system provide certain technical issues during the operation of the utility grid. Such technical issues are listed below:-

a) Steady state and transient over or under voltages at the point of common coupling (PCC).
b) Protection malfunctions.
c) Increase in short-circuit levels.
d) Power Quality issues.
e) Low inertia of interfacing inverters/converters.

1.5 SCOPE OF WORK

In this thesis, control algorithm is developed for the integration of multiple sources to LV grids. These multiple sources, referred to as RESs are intermittent in nature. These RESs are connected to the utility grid at the PCC via power electronic interface which have very low inertia due to the fast control of the static switches. In this thesis, control algorithm is developed for creating virtual inertia in the PE interface system such that during intermittency in DG, power flow from the utility grid do not make

sudden transitions thus ensuring system stability. This thesis also presents that the reactive power requirement of the load is fulfilled by supplying reactive component locally through STATCOM. Thus control algorithm is developed for improving the power quality of the system.

1.6 ORGANIZATION OF THESIS

The thesis work is presented in the different chapters. An overview of the chapters is as follows:

Chapter II: It gives an overview of literature survey. This chapter begins with the overview of RES and OE interface with RES. An overview on microgrids and its different modes of the operation is presented. Technical challenges related to micro grids are discussed henceforth. Lastly, literature review on control strategies for microgrids is depicted, discussing tradition droop control in brief.

Chapter III: This chapter deals with the mathematical modelling involved while developing control algorithms for the stable, reliable operation of microgrids. Mathematical modelling involves representation of phasor in α-β frame, representation of phasor in d-q frame, Hysteresis current control method is then discussed henceforth. This chapter concludes with the mathematical modelling and design of PLL and mathematical representation of droop controller used in control algorithm.

Chapter IV: This chapter represents the system configuration and discusses the operation of utility system during intermittent behaviour of DG when:

a) Inertial support is not provided.
b) Inertial support is provided.

The control algorithm developed for creating the virtual inertial by providing droop controller is discussed in this chapter. This chapter discusses the control algorithm for improving system stability and power system quality as well.

Chapter V: This chapter represents the analysis and results of the system done under MATLAB simulate environment. MATLAB simulations for grid connections DG under various load conditions have been presented in this chapter.

Chapter VI: This chapter present the main conclusions based on the proposed work and also enlist the suggestions for the further work based on the present investigation.

CHAPTER 2
LITERATURE SURVEY

2.1 GENERAL INTRODUCTION

Generation of electricity from renewable energy sources has been the research area of interest that is exponentially increasing in the past decade. Generally in conventional power system electricity generated from thermal power plants, nuclear power plants etc. located at remote locations is fed to the distribution network through transmission lines. Thus in conventional power distribution system, a single source is feeding a network of downstream feeders [1] with the penetration of distributed generation, this conventional grid's structure has broken. Therefore, a lot of research is going on to study the dynamic analysis of DG and its integration with conventional power system.

This chapter presents the literature review on the renewable energy sources, power electronics interface for integration with RES, issues with PE interface for grid integration of RES. Further, an overview on microgrids and its operations in various modes is presented.

2.2 RES AND PE INTERFACE WITH RES

In order to improve power supply reliability and quality, integration of DG using renewable energy sources at the distribution site is gaining importance. This increasing penetration of renewable energy sources and DG's require new strategies for the operation and management of the electricity grid. The power electronic technology plays an important role in distributed generation and in integration of renewable energy sources into the electric grid. [2]

Power Electronics is undergoing fast evolution due to two factors:

1) Development of fast semiconductor switches capable of switching quickly and handling high powers.
2) Real- Time Computer Controllers which can implement complex and advanced control algorithms.

Thus due to development of power electronic technology it has been possible to develop power electronics interface for the highest projected turbine rating for generation of electricity through wind for integration of solar panels for the generation of electricity through solar energy. With advent of power electronics technology it has been possible to optimize energy conversion and transmission and control reactive power; minimize harmonic distortion; increase reliability and achieve a wide power range with high efficiency at low cost.

2.3 MICROGRIDS: AN OVERVIEW AND ITS MODE OF OPERATIONS

A microgrid is defined as an electric power distribution system having capability of generation of electricity locally using renewable energy sources; having various DG's; energy storage systems and loads which can operate both in grid-connected mode and in islanded mode, when derived. Power electronics interface between the micro grid buses and storage units detect the mode of operation of micro grid, allow seamless transition between the modes, flow of power in both directions while maintaining system stability and power quality and thus ensuring system reliability.

2.4 MICROGRIDS: TECHNICAL CHALLENGES

Various technical issues occur due to integration of renewable energy sources into the grid. Issues arise in the areas of power quality, harmonic oscillations, voltage stability, reliability, protection and control. The foremost power quality hitches which affect the utility grid power quality are voltage unbalance, increased reactive power demand, harmonics and frequency deviation which can be improved by suitable operation of power electronic devices. Control algorithms have to be developed to improve voltage sags/swells and unbalances and to improve the power quality on an acceptable level.

2.4.1 Stability Issues in Microgrids

Due to high penetration of DGs and RESs, stability issues arise in the microgrids. These stability issues are depicted below:

i) **Low inertia of the power electronic based converters used in the microgrid:** In conventional power grids, the inertial support from the rotating mass of the

synchronous generators play an important role for maintaining grid frequency during the transient periods. In microgrids, DGs do not render inertial backup during power grid disturbances as they are integrated to the main grid through power electronic based converters which results in lower system inertia. This lower system inertia contributes to voltage and frequency instabilities during transient periods.

ii) **Low voltage stability due to lower power distribution support:** Power electronic converters in DGs are operated in current control mode when DGs are connected in grid-connected mode. Because of low capacity of DGs as compared to the utility grid, power sharing support from DGs is much less compared to that of traditional power plants. Moreover, traditional power plants can meet the increased power requirements with the kinetic energy stored in the rotating mass of synchronous generators during various eventualities. Thus, high penetration of DGs can deteriorate the voltage profile immunity during various power system outages.

2.4.2 Harmonics in Microgrids

The harmonics arise due to the operation of power electronics converters. In order to reduce harmonics losses, harmonic currents need to be reduced. The harmonic voltage and current must be limited to the acceptable levels at the point of common coupling.

2.5 MICROGRIDS: CONTROL STRATEGIES WITH ENERGY STORAGE SYSTEMS

Power networks are undergoing a transition from the traditional centralized generation model towards decentralized network of RES and energy storage (ES) systems [5]. However, intermittent generation using RES and bi-directional flow of power through PE converters introduce challenges for the network power quality and stability of the network. A microgrid consists of set of generation sources, loads and energy storage systems that are co-ordinated to achieve autonomous operations.

The hierarchical microgrid control model has three levels:-

i) The primary control level is responsible for load sharing between the microgrid sources, to maintain stability and autonomous operations (having time-scales on the

order of 10 to 100ms). The primary control method is the decentralized droop control which provides load sharing between the sources. However, droop control introduces a trade-off between load sharing accuracy and microgrid power quality, in the form of voltage/frequency offsets.

ii) The centralized secondary control level restores the voltage/frequency offsets introduced by primary control (having time scales on the order of 1 to 10 sec). The secondary control can also used to correct the primary control load sharing ratios.

iii) The tertiary control level is used to solve the microgrid optimal power flow (OPF) problem (having time scales of the order of 10-15 min). The control is based on a static power model.

2.5.1 Traditional Droop Control

The standard primary control strategy is decentralized droop control which is responsible for load sharing between sources which are interfaced with the microgrid through power electronic converters. Here basic traditional droop control is discussed in detail.

AC microgrids which have reactive impedance have real power flows dependent on bus voltage angles and reactive power flows dependent on bus voltage magnitudes. This depicts the traditional f-P, V-Q droop control. In f-P droop control; converters reduce their frequency in proportion to the real output power and their voltage in proportion to the reactive output power. Thus, in steady state; they share real and reactive load in inverse proportion to their droop coefficient. Low voltage microgrids have resistive lines in which case V-P, f-Q droop control is used. Virtual impedance is introduced to reduce the coupling between real and reactive power flows.

Thus, various control strategies for microgrids have been presented and discussed in order to meet the power quality and stability challenges of the electric network.

2.6 CONCLUSION

From the above literature it is evident that a lot of research is going on in the field of power electronics in order to generate electricity using renewable energy sources. With the integration of more renewable energy sources in the utility grid and due to the intermittent nature of RES, RES based DGs connected in the microgrid pose a lot of challenges to the

existing conventional grid: major problem being the low inertia of power electronic converters. In order to meet these challenges various control algorithms and control strategies developed are discussed in this chapter.

Chapter 3
MATHEMATICAL MODELLING

3.1 GENERAL INTRODUCTION

This chapter gives a detailed description of the mathematical tools and techniques used in the thesis work. All calculations are performed in $\alpha\beta$ −frame and dq – frame of reference as it is easier to analyze the system in dq – frame of reference rather than abc – frame of reference. All voltages and currents in abc – frame of reference are transformed into dq – frame of reference. Detailed analysis of various techniques such as hysteresis current control and PLL has been done in this chapter by deriving mathematical relations required to obtain the conditions. This chapter concludes with the mathematical analysis of droop control.

3.2 $\alpha\beta$ −FRAME REPRESENTATION OF A SPACE PHASOR

A space phasor expressed in polar coordinate system, is a complex valued function of time. It is represented by amplitude and phase of the system. This representation is used in expressing the dynamics of system variables in terms of amplitude and phase of the system. However, for designing and implementing control algorithms represented as real – valued functions of time, it is preferred to map space phasors and space-phasor equations in the Cartesian coordinate system.

Cartesian coordinate system also known as $\alpha\beta$ − frame is being presented here in detail.

3.2.1 $\alpha\beta$ − Frame Representation

Let us consider a space phasor $\vec{g}(t)$ given by eq.3.1 as:

$$\vec{g}(t) = \frac{2}{3}\left[e^{j0}g_a(t) + e^{j2\pi/3}g_b(t) + e^{j4\pi/3}g_c(t)\right] \quad 3.1$$

where, $g_a + g_b + g_c = 0$

$\vec{g}(t)$ decomposed into real and imaginary components is expressed in eq.3.2 as : -

$$\vec{g}(t) = g_\alpha(t) + jg_\beta(t) \qquad 3.2$$

Where $g_\alpha(t)\ and\ g_\beta(t)$ refers to $\alpha - axis$ components and $\beta - axis$ components of $\vec{g}(t)$, respectively.

Equating eq. 3.1 and eq.3.2 gives real and imaginary parts: -

$$\begin{bmatrix} g_\alpha(t) \\ g_\beta(t) \end{bmatrix} = \frac{2}{3} A \begin{bmatrix} g_a(t) \\ g_b(t) \\ g_c(t) \end{bmatrix} \qquad 3.3$$

Where, $A = \begin{bmatrix} 1 & -1/2 & -1/2 \\ 0 & \sqrt{3}/2 & -\sqrt{3}/2 \end{bmatrix}$

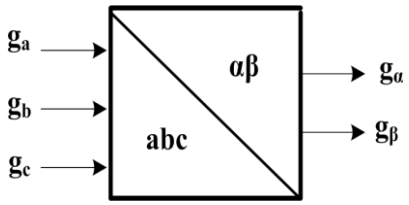

Fig. 3.1 Block diagram of abc/ αβ transformation

Thus, Projections of $\vec{g}(t)$ on real-axis and imaginary axis are represented as respectively as $g_\alpha(t)\ and\ g_\beta(t)$ as depicted in eq. 3.2.

g_{abc} expressed in terms of $g_{\alpha\beta}$ is represented as: -

$$\begin{bmatrix} g_a(t) \\ g_b(t) \\ g_c(t) \end{bmatrix} = A^T \begin{bmatrix} g_\alpha(t) \\ g_\beta(t) \end{bmatrix}$$

Representation of space phasor $\vec{g}(t)$ in $\alpha\beta$-frame is depicted below where;

$$\hat{g}(t) = \sqrt{g_\alpha^2(t) + g_\beta^2(t)}$$

$$\cos\theta = \frac{g_\alpha(t)}{\hat{g}(t)} = \frac{g_\alpha(t)}{\sqrt{g_\alpha^2(t) + g_\beta^2(t)}}$$

$$\sin\theta = \frac{g_\beta(t)}{\hat{g}(t)} = \frac{g_\beta(t)}{\sqrt{g_\alpha^2(t) + g_\beta^2(t)}}$$

$$\left.\begin{aligned} g_\alpha(t) &= \hat{g}(t)\cos\theta \\ g_\beta(t) &= \hat{g}(t)\sin\theta \end{aligned}\right] \qquad 3.4$$

In eq.3.4, $g_\alpha \; and \; g_\beta$ represent sinusoidal functions of time having amplitude $\hat{g}(t)$ and frequency $w = {}^{d\theta}/_{dt}$.

Now the objective is to determine a system that receives space phasor $\vec{g}(t)$ as an input and produces space phasor $\overrightarrow{g'}(t)$ as output corresponding to a new 3-phase signal with the following properties:

The amplitude of $g'(t)$ is $A(t)$ times that of corresponding $g(t)$, where $A(t)$ is an arbitrary function of time.

Phase angle of each component of $g'(t)$ is shifted by $\varphi(t)$ w.r.t. corresponding component of $g(t)$, where $\varphi(t)$ is an arbitrary function of time.

Thus $g'(t)$ is represented in eq.3.5 as: -

$$g'(t) = \vec{g}(t)A(t)e^{j\varphi(t)} \qquad 3.5$$

$g'(t)$ as space-phasor has the property of phase-shifter/scalar as it enables desired phase shift and amplitude scaling.

$g'(t)$ represented in $\alpha\beta -$ frame of reference is expressed in eq.3.6 as

$$\begin{bmatrix} g'_\alpha(t) \\ g'_\beta(t) \end{bmatrix} = A(t) \begin{bmatrix} cos\varphi & -sin\varphi \\ sin\varphi & cos\varphi \end{bmatrix} \begin{bmatrix} g_\alpha(t) \\ g_\beta(t) \end{bmatrix} \qquad 3.6$$

3.2.2 Formulation of Power in $\alpha\beta$ −frame

Let us assume

$$\vec{V}(t) = V_\alpha(t) + jV_\beta(t)$$

$$\vec{I}(t) = I_\alpha(t) + jI_\beta(t)$$

The instantaneous real and reactive components of power are calculated in eq.3.7 as: -

$$\left.\begin{aligned} P(t) &= \tfrac{3}{2}\left[V_\alpha(t)I_\alpha(t) + V_\beta(t)I_\beta(t)\right] \\ Q\,(t) &= \tfrac{3}{2}\left[-V_\alpha(t)I_\alpha(t) + V_\beta(t)I_\beta(t)\right] \end{aligned}\right\} \quad 3.7$$

3.2.3 Control in $\alpha\beta$ −frame

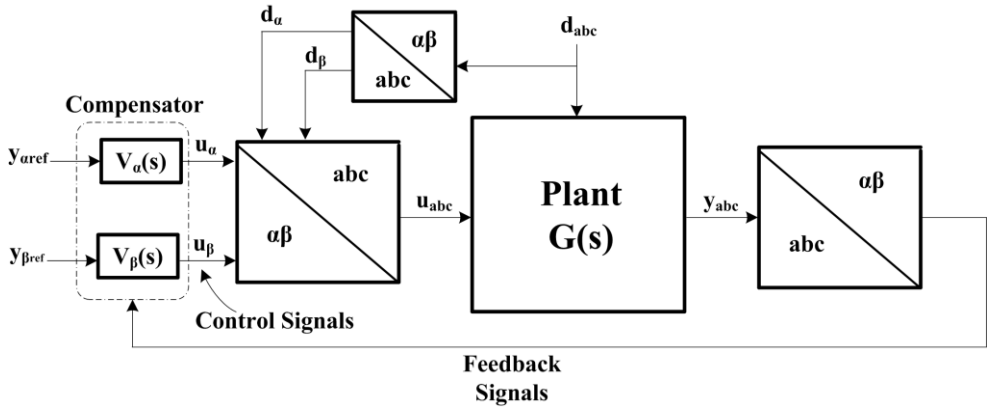

Fig.3.2 Block diagram of the control scheme of 3 – phase system in $\alpha\beta$ − frame

Fig.3.2 represents the block diagram of the control scheme of 3 – phase system in $\alpha\beta$ − frame. Here $G(s)$ represents the transfer function having u_{abc} as the control input and y_{abc} as the system output which are decided based on the application and control operation requirements. $G(s)$ describes the relation between input and output signal.

d_{abc} represents the disturbance signal present in the system. The key objective of the control system is to control y_{abc} when u_{abc} is applied as input to the system in the presence of disturbance signal d_{abc}.

In order to exercise the control in $\alpha\beta$ − frame of reference, based on the reference signal, feedback and feed-forward signals, a set of compensators $k_\alpha(s)$ and $k_\beta(s)$ generate the control signals $u_\alpha$and $u_\beta$that are transformed back to u_{abc} and is applied to the plant.

In order to design the compensators, the dynamics of the plant must be formulated in $\alpha\beta$ −frame of reference. In case a symmetrical plant is represented in $\alpha\beta$ −frame of reference, compensators $k_\alpha(s)$ and $k_\beta(s)$ represent two decoupled sub-systems that can be controlled independently. But in case of asymmetrical system; α −axis and β −axis sub-systems are coupled. So compensators cannot be split. However, under special conditions using various appropriate feed-forward techniques, α −axis and β −axis dynamics may be decoupled.

It should be taken into account that $y_{\alpha\, ref}$ and $y_{\beta\, ref}$ represent sinusoidal functions of time. To ensure satisfactory tracking performance, either the closed loop control system has a large bandwidth or the compensators include complex-conjugate poles at the frequency of the command signals. Therefore, for variable frequency applications such control systems are not suitable. For such applications, control scheme based on dq-frame of reference is adopted.

3.3 REPRESENTATION OF A SPACE PHASOR IN *dq*- FRAME OF REFERENCE

3.3.1 dq – frame representation

For the space phasor; $\vec{g} = g_\alpha + jg_\beta$, $\alpha\beta\ to\ dq$ frame transformation is defined by eq.3.8 as :

$$g_d + jg_q = (g_\alpha + jg_\beta)e^{-j\epsilon(t)} \qquad 3.8$$

- $\epsilon(t)$ being the angle that represents phase shift in $\vec{g}(t)$

$$\vec{g} = g_\alpha + jg_\beta = e^{j\epsilon(t)}(g_d + jg_q) \qquad 3.9$$

Let $\vec{g}$ be represented in general form in eq.3.10 as : -

$$\vec{g} = g_\alpha + jg_\beta = \hat{g}(t)e^{j[\theta_o + \int \omega(\tau)d\tau]} \quad 3.10$$

Where $\omega(t)$ represents time - varying frequency and θ_o represents initial phase angle of $\vec{g}(t)$.

$\epsilon(t) = \epsilon_o + \int \omega(\tau)\, d\tau$,

dq-frame representation of $\vec{g}(t)$ is expressed in eq.3.11 as:

$$g_d + jg_q = \hat{g}(t)e^{j(\theta_o - t_o)} \quad 3.11$$

Above eq.3.11 represents stationary quantity and therefore, the constituents of its corresponding three phase signals are DC quantities.

It must be noted that it is not necessary that $\theta(t) and\ \epsilon(t)$ are equal but it must be ensured that $\frac{d\theta(t)}{dt} = \frac{d\epsilon(t)}{dt}$

Therefore, from eq. 3.9, $\vec{g}$ can be considered as a vector having $g_d\ and\ g_q$ as components of the vector $\vec{g}$ in the coordinate system that is rotated by $\epsilon(t)$ with respect to $\alpha\beta -$frame. This rotating frame of reference is known as *dq*-frame of reference.

The speed of rotation of the dq-frame of reference is selected to be equal to that of $\vec{g}$.

On the basis of Euler's identity, eq. 3.8 can be represented as: -

$$\begin{bmatrix} g_d(t) \\ g_q(t) \end{bmatrix} = R[\epsilon(t)] \begin{bmatrix} g_\alpha(t) \\ g_\beta(t) \end{bmatrix} \quad 3.12$$

Where, $\mathrm{R}[\epsilon(t)] = \begin{bmatrix} \cos\ \epsilon(t) & \sin\ \epsilon(t) \\ -\sin\ \epsilon(t) & \cos\ \epsilon(t) \end{bmatrix}$

Similarly, *dq*- to $\alpha\beta -$ frame transformation is expressed in eq.3.13 as:

$$\begin{bmatrix} g_\alpha(t) \\ g_\beta(t) \end{bmatrix} = R^{-1}[\epsilon(t)] \begin{bmatrix} g_d(t) \\ g_q(t) \end{bmatrix} \quad 3.13$$

Where, $R^{-1}[\epsilon(t)] = R[-\epsilon(t)] = \begin{bmatrix} \cos\ \epsilon(t) & -\sin\ \epsilon(t) \\ \sin\ \epsilon(t) & \cos\ \epsilon\,(t) \end{bmatrix}$

A direct transformation from abc-frame to dq-frame can be obtained as: -

$$\begin{bmatrix} g_d(t) \\ g_q(t) \end{bmatrix} = \frac{2}{3} T\,[\epsilon(t)] \begin{bmatrix} g_a(t) \\ g_b(t) \\ g_c(t) \end{bmatrix} \qquad 3.14$$

Where; $T\,[\epsilon(t)] = R[\epsilon(t)]A = \begin{bmatrix} \cos\epsilon(t) & cos\left[\epsilon(t) - {}^{2\pi}/_{3}\right] & cos\left[\epsilon(t) - {}^{4\pi}/_{3}\right] \\ \sin\epsilon(t) & sin\left[\epsilon(t) - {}^{2\pi}/_{3}\right] & sin\left[\epsilon(t) - {}^{4\pi}/_{3}\right] \end{bmatrix}$

A direct transformation from dq-frame to abc-frame represented in eq.3.15 as: -

$$\begin{bmatrix} g_a(t) \\ g_b(t) \\ g_c(t) \end{bmatrix} = T\,[\epsilon\,(t)]^T \begin{bmatrix} g_d(t) \\ g_q(t) \end{bmatrix} \qquad 3.15$$

Where; $T\,[\epsilon\,(t)]^T = A^T R[-\epsilon\,(t)] = \begin{bmatrix} \cos\,[\epsilon\,(t)] & \sin\,[\epsilon\,(t)] \\ cos\left[\epsilon\,(t) - {}^{2\pi}/_{3}\right] & sin\left[\epsilon\,(t) - {}^{2\pi}/_{3}\right] \\ cos\left[\epsilon\,(t) - {}^{4\pi}/_{3}\right] & sin\left[\epsilon\,(t) - {}^{4\pi}/_{3}\right] \end{bmatrix}$

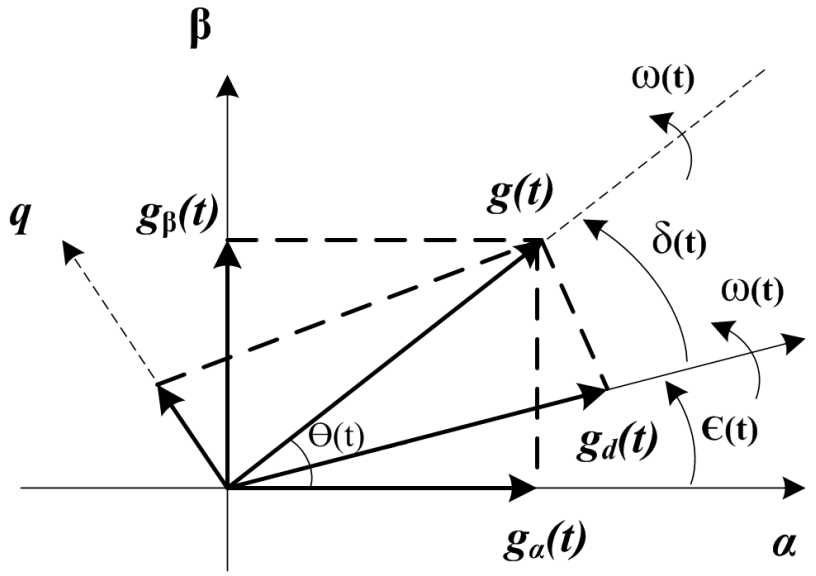

Fig.3.3 Phasor diagram representation of $\alpha\beta$ − frame and dq – frame of reference

Fig.3.3 represents the phasor diagram representation of $\alpha\beta$ − frame and dq – frame of reference.

Based on Fig. 3.3

$$\hat{g}(t) = \sqrt{g_d^2(t) + g_q^2(t)}$$

$$\cos\ [\delta(t)] = \frac{g_d(t)}{\hat{g}(t)} = \frac{g_d(t)}{\sqrt{g_d^2(t) + g_q^2(t)}}$$

$$\sin\ [\delta(t)] = \frac{g_q(t)}{\hat{g}(t)} = \frac{g_q(t)}{\sqrt{g_d^2(t) + g_q^2(t)}}$$

$$\theta(t) = \epsilon(t) + \delta(t)$$

3.3.2 Formulation of Power in *dq*- Frame

$$\vec{V}(t) = (V_d + jV_q)e^{j\epsilon(t)}$$

$$\vec{I}(t) = (I_d + jI_q)e^{j\epsilon(t)}$$

$$\left.\begin{aligned} P(t) &= \tfrac{3}{2}\left[V_d(t)I_d(t) + V_q(t)I_q(t)\right] \\ Q(t) &= \tfrac{3}{2}\left[-V_d(t)I_d(t) + V_q(t)I_q(t)\right] \end{aligned}\right\} \quad 3.16$$

Eq. 3.16 depicts that if $V_q = 0$, then real and reactive components of power are proportional to $I_d\ and\ I_q$ respectively. The above property is used in the control algorithms of grid-connected three-phase VSC systems.

3.3.3 Control in *dq*- frame of reference

In $\alpha\beta$ −frame of reference feed – forward signal, feedback signal and control signal are sinusoidal functions of time. The control system represented in d-q frame of reference is an extension of control system represented in $\alpha\beta$ −frame of reference. In dq-frame, compensators process DC signals ($D_{dq}\ and\ Y_{dq}$) rather than sinusoidal signals and provide V_{dq} control signal.

In fig. 3.3, $\epsilon(t)$ represents the angle between $\alpha\beta -$ frame of reference and $dq -$ frame of reference.

$\epsilon(t) = \epsilon_o(t) + \int \omega(\tau)d\tau$, where $\omega(t)$ is the frequency and ϵ_o is a constant. In the special case of VSC system, $\omega(t)$ is equal to AC system operating frequency, ω_o and $\epsilon(t) = \epsilon_o(t) + \omega_o t$.

3.4. HYSTERESIS CURRENT CONTROL METHOD

Hysteresis current control is a method used to generate the required triggering pulses for a power electronic inverter by comparing the error signal with that of the hysteresis band by selecting suitable relays. It is used to control the voltage source inverter (VSI) such that the output current that is generated from the battery energy storage system (BESS) will follow the reference current waveform.

The switches of the voltage source inverter are controlled asynchronously to ramp the current through the inductor up and down, such that it follows the reference current waveform. Hysteresis current control is a simple and robust control method for implementation in the real time.

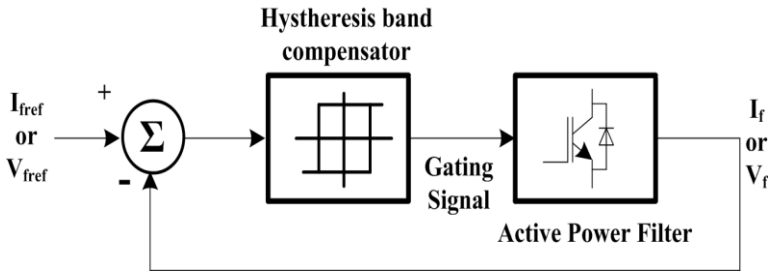

Fig.3.4 Block diagram representation of Hysteresis Current control

Fig.3.4 represents block diagram of hysteresis current control in which gating signals are generated by comparing the error signal with that of hysteresis band and in turn are used to control the voltage source inverter.

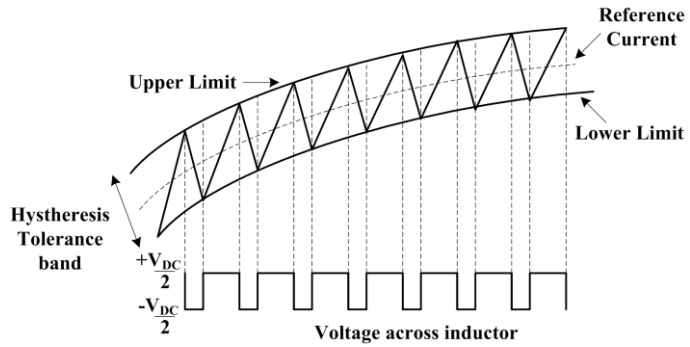

Fig.3.5 Hysteresis control band representation

Fig.3.5 depicts the ramping of the current between the two limits where the upper hysteresis limit is the addition of the reference current and the average value of the hysteresis tolerance band and lower hysteresis limit is the subtraction of the reference current and the average value of the same tolerance band. This ramping current corresponds to the actual current of the inductor. When the ramping current waveform touches the upper hysteresis band it triggers a negative edge pulse of amplitude($-V_{DC}$) making a transition from $+V_{DC}/2$ to $-V_{DC}/2$. Similarly when the ramping current waveform touches the lower hysteresis band it triggers a positive edge pulse of amplitude($+V_{DC}$) making a transition from $-V_{DC}/2$ to $+V_{DC}/2$.

As per the operating principle of the inverter, the switching pulses of the switches in each leg of the inverter determine the output voltages of each phase of the inverter. Thus, the switching gates for the battery energy storage system (BESS) can be obtained which controls the voltage of voltage source inverter. The voltages across the inductors determine the switching frequency and the frequency can be altered by adjusting the width of the hysteresis tolerance band.

3.5 PHASE LOCKED LOOP (PLL)

Representation of a space phasor $\vec{g}(t)$ in dq- frame is expressed below in eq.3.17 as: -

$$\vec{g}(t) = g_\alpha + jg_\beta \qquad 3.17$$

dq- to $\alpha\beta$ − transformation is given by eq.3.18 as: -

$$g_d + jg_q = \vec{g}(t)e^{-j\epsilon(t)} \quad 3.18$$

Here, $-\epsilon(t)$ represents the phase shift in $\vec{g}(t)$.

Let us assume that AC system voltage in the VSC system is expressed by eq.3.19 as: -

$$\left.\begin{aligned} V_{sa}(t) &= \hat{V}_s(\omega_o t + \theta_0) \\ V_{sb}(t) &= \hat{V}_s\left(\omega_o t + \theta_0 - {}^{2\pi}/_{3}\right) \\ V_{sc}(t) &= \hat{V}_s\left(\omega_o t + \theta_0 - {}^{4\pi}/_{3}\right) \end{aligned}\right] \quad 3.19$$

where, $\hat{V}_s$ represents the peak line to neutral voltage, ω_o represents the frequency of AC system and θ_0 represents initial phase angle of the source.

Space phasor equation of V_{s-abc} is:

$$\vec{V_s}(t) = -j\hat{V}_s e^{j(\omega_o t + \theta_o)} \quad 3.20$$

Dynamics of AC side of VSC system of Fig.3.6 is described by the following equation:

$$L\frac{d\vec{\imath}}{dt} = -(R + r_{on})\vec{\imath} + \vec{V}_t - \vec{V}_s \quad 3.21$$

Substituting eq. 3.20 in eq. 3.21

$$L\frac{d\vec{\imath}}{dt} = -(R + r_{on})\vec{\imath} + \vec{V}_t + j\hat{V}_s e^{j(\omega_o t + \theta_o)}$$

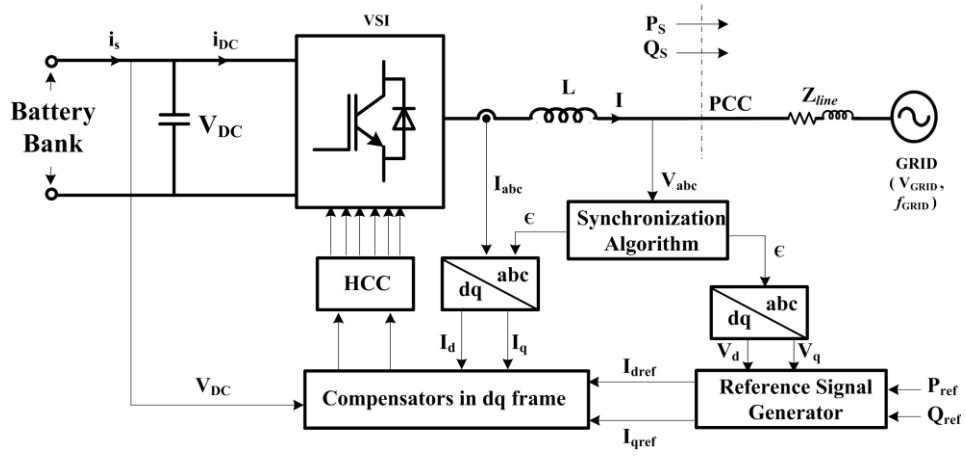

Fig.3.6 Schematic diagram of current – controlled real/reactive - power controller in dq - frame

Now, substituting $\vec{\imath} = i_{dq}e^{j\epsilon}$ and $\overrightarrow{V_t} = V_{t_{dq}}e^{j\epsilon}$, we get;

$$L\frac{d(i_{dq}e^{j\epsilon})}{dt} = -(R + r_{on})i_{dq}e^{j\epsilon} + V_{t_{dq}}e^{j\epsilon} + j\hat{V}_s e^{j(\omega_o t+\theta_o)}$$

Where, $f_{dq} = f_d + jf_q$

$$L\frac{d(i_{dq})}{dt} = +V_{t_{dq}} - (R + r_{on})i_{dq} - j\left(L\frac{d\epsilon}{dt}\right)i_{dq} + j\hat{V}_s e^{j(\omega_o t+\theta_o)}$$

3.22

Decomposing eq. 3.22 into real and reactive components,

$$L\frac{di_d}{dt} = \left(L\frac{d\epsilon}{dt}\right)i_q + V_{t_d} - (R + r_{on})i_d - \hat{V}_s sin(\omega_o t + \theta_o - \epsilon) \quad 3.23$$

$$L\frac{di_q}{dt} = -\left(L\frac{d\epsilon}{dt}\right)i_d + V_{t_q} - (R + r_{on})i_q + \hat{V}_s cos(\omega_o t + \theta_o - \epsilon) \quad 3.24$$

Now, we introduce new control variable ω in eq. 3.23 and eq. 3.24 as $= \frac{d\epsilon}{dt}$. This gives;

$$L\frac{di_d}{dt} = L\omega(t)i_q - (R + r_{on})i_d + V_{t_d} - \hat{V}_s sin(\omega_o t + \theta_o - \epsilon) \quad 3.25$$

$$L\frac{di_q}{dt} = L\omega(t)i_d - (R + r_{on})i_q + V_{t_q} + \hat{V}_s cos(\omega_o t + \theta_o - \epsilon) \quad 3.26$$

$$\frac{d\epsilon}{dt} = \omega(t) \quad 3.27$$

in eq. 3.25, 3.26 and 3.27; $i_d , i_q \; and \; \epsilon$ represent the state variables; $V_{td} , V_{tq} \; and \; \omega$ represent the control inputs. The system described in eq. 3.25- eq. 3.27 is non-linear because of the presence of the terms $\omega i_d , \omega i_q, \cos(\omega_o t + \theta_o - \epsilon)$ and $\sin(\omega_o t + \theta_o - \epsilon)$.

This discussion depicts that with the proper selection of the values of $\omega \; and \; \epsilon$ *dq*-frame of reference can be very useful.

For the VSC system in Fig.3.6, if $\omega = \omega_o , \epsilon(t) = \omega_o t + \theta_o$ then eq. 3.25 and eq. 3.26 takes the form:

$$L\frac{di_d}{dt} = L\omega_o i_q - (R + r_{on})i_d + V_{t_d} \quad 3.28$$

$$L\frac{di_q}{dt} = L\omega_o i_d - (R + r_{on})i_q + V_{t_q} \quad 3.29$$

which gives the description of the second-order linear system that is excited by the constant input $\hat{V}_s$. Thus, if $V_{t_d}\ and\ V_{t_q}$ are DC variables, $i_d\ and\ i_q$ also represent DC variables in the steady state. The mechanism to ensure $\epsilon(t) = \omega_o t + \theta_o$ is referred to as the Phase Locked Loop (PLL).

Now, substituting eq. 3.20 in eq. 3.18

$$V_{S_d} = \hat{V}_s sin(\omega_o t + \theta_o - \epsilon) \quad 3.30$$

$$V_{S_q} = -\hat{V}_s cos(\omega_o t + \theta_o - \epsilon) \quad 3.31$$

Therefore, eq. 3.25 and eq. 3.26 can be represented by eq.3.32 and eq.3.33 as: -

$$L\frac{di_d}{dt} = L\omega(t)i_q - (R + r_{on})i_d + V_{t_d} - V_{S_d} \quad 3.32$$

$$L\frac{di_q}{dt} = L\omega(t)i_d - (R + r_{on})i_q + V_{t_q} - V_{S_q} \quad 3.33$$

$$\frac{d\epsilon}{dt} = \omega(t) \quad 3.34$$

$$\overrightarrow{V_{S_{dq}}} = -j\hat{V}_S e^{j(\omega_o t + \theta_o)} e^{-j\epsilon} = -j\hat{V}_S e^{j(\omega_o t + \theta_o - \epsilon)}$$

On the basis of eq. 3.30, $\epsilon(t) = \omega_o t + \theta_o$ corresponds to $V_{S_d} = 0$. Therefore, we devise a mechanism to regulate V_{S_d} at zero. This can be achieved based on the following feedback law: -

$$\omega(t) = H(p)\, V_{S_d}(t) \quad 3.35$$

Where $H(p)$ represents a linear transfer function,

$p = {}^{d(.)}/_{dt}$ is a differentiation operator.

Substituting eq. 3.30 and eq. 3.34 in eq. 3.35 gives eq.3.36 as:

$$\frac{d\epsilon}{dt} = H(p)\,\hat{V}_s\,sin\,(\omega_o t + \theta_o - \epsilon\,) \qquad 3.36$$

Eq. 3.36 describes a non-linear dynamic system known as PLL. The operation of the Phase Locked Loop (PLL) is to regulate ϵ at $\omega_o t + \theta_o$.

If the PLL tracks $\omega_o t + \theta_o$; the term $\omega_o t + \theta_o - \epsilon$ is close to zero; therefore;

$$\frac{d\epsilon}{dt} = \hat{V}_s\,H(p)\,(\omega_o t + \theta_o - \epsilon) \qquad 3.37$$

Eq. 3.37 gives a representation of a classical feedback control loop in which $\omega_o t + \theta_o$ represents the reference input, ϵ represents the output and $\hat{V}_s\,H(s)$ represents the transfer function of the effective compensator. Control block diagram of the phase locked loop is shown in Fig. 3.7.

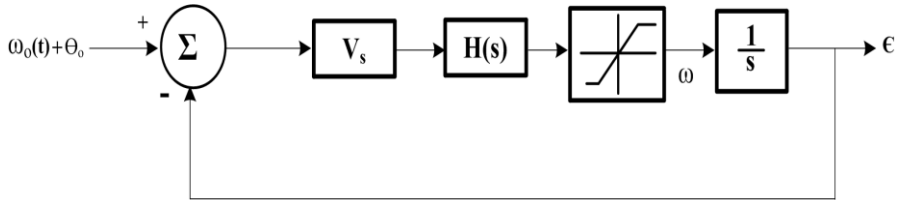

Fig.3.7 Control Block of PLL

3.6 DROOP CONTROL

The active and reactive power drawn to the bus is given by the following relations:

$$P_i = \frac{VE_i\,sin\emptyset}{X} \qquad 3.38$$

$$Q_i = \frac{VE_i cos\emptyset - V^2}{X} \qquad 3.39$$

Where X represents the output reactance of the power inverter, $\emptyset$ represents the phase angle between the output voltage of the power inverter and the voltage of the common bus, and E_i and V represent the amplitude of the output voltage of the inverter and the

grid voltage, respectively. Above equations depict that active power depends on the power angle and reactive power depends on the amplitude of the output voltage such that the rate at which power inverters inject the active current can be controlled by controlling the slope of the equation given below:

$$I_i = \frac{P_i}{V} = \frac{E_i \sin\emptyset}{X} \qquad 3.40$$

The slope of the above equation also known as droop slope is given by the equation below:

$$m_i = \frac{E_i}{X} \qquad 3.41$$

3.7 CONCLUSION:

In this chapter, various mathematical tools and techniques used in the control algorithm for the operation of power electronic inverters in the system are discussed in detail. The mathematical tools depicted in this chapter helps analyzing the system in a much simpler way and thus make implementation of the algorithms conveniently.

CHAPTER-4
SYSTEM CONFIGURATION AND CONTROL ALGORITHM

4.1 GENERAL INTRODUCTION

This chapter proposes the system configuration for the operation of the micro grid in the grid connected mode in distribution network. In this chapter the control algorithm is designed for developing virtual inertia of the inverter using the droop control during intermittent operation DG in grid connected mode, avoiding sudden transition of current in the grid side. Proposed control algorithm allows smooth transition of the power flow from the grid, thus ensuring system stability. The proposed control algorithm maintains unity power factor at the grid side ensuring maximum power utilization from the grid. The designed algorithm thus ensures system stability alongwith enhancement of power quality during intermittent operation of DG operating in grid connected mode.

4.2 SYSTEM CONFIGURATION

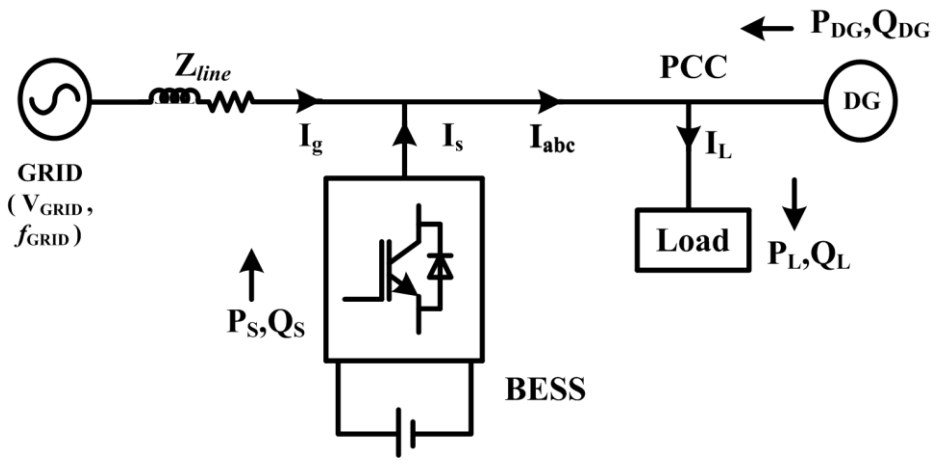

Fig.4.1 System Configuration

Fig 4.1 represents the block diagram of a radial distribution network in which an infinite grid is connected to a load having real and reactive power requirement of 7 kW and 3.5 kVAR respectively. DG having capacity of 3.5 kW, a constant current source acting as a source of real power is connected to the distribution network at the point of common coupling (PCC) for supplying real power to the local loads. Battery energy storage system (BESS), designed as per system requirement is connected in shunt at the load side at PCC operating in current controlled mode. During intermittent operation of DG, BESS delivers or absorbs real power as per the system requirement so as to ensure system stability at PCC. Reactive power demand of the load is catered locally by BESS as BESS supplies or absorbs reactive power as per the requirement of the load such the unity power factor(UPF) is maintained at the grid side.

4.3 BASIC OPERATION

4.3.1 Case A: Without Battery Energy Storage System (BESS)

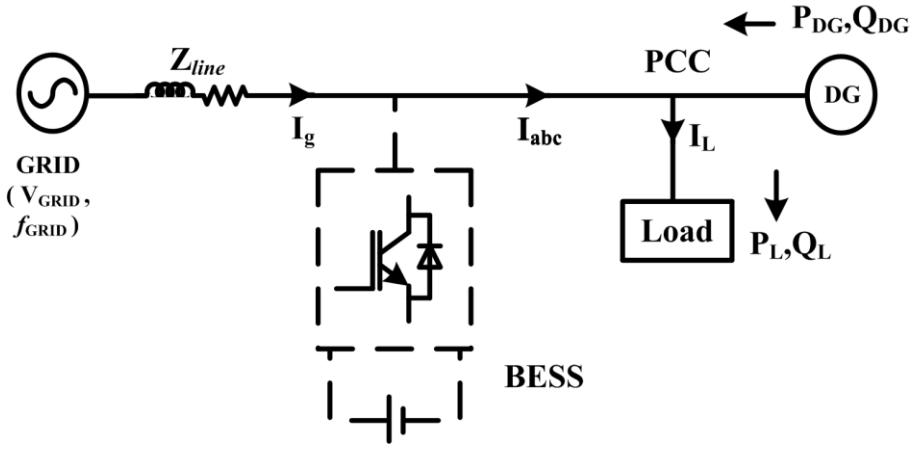

Fig.4.2 System Configuration without BESS

Fig.4.2 presents system configuration when BESS is not connected to the utility grid. In this system configuration, an infinite grid is present alongwith DG having capacity of 3.5kW and load having real and reactive power requirement of 7 kW and 3.5 kVAR. In steady state operation real power requirement of the load is being shared by DG and grid; DG providing its maximum available real power at that instant of time.

The reactive power requirement of the load is being catered by the grid. Real power flowing from the grid changes abruptly with the sudden transitions in the real power flow from the DG due to intermittency of RES. In weak grids or LV grids where R/X ratio is high, voltage at PCC fluctuates with the current flowing from the grid. Due to intermittent nature of RES & power requirement of the load being constant, power flow from the grid changes abruptly which affects the stability of the grid.

4.3.2 Case B: With Battery Energy Storage System (BESS)

Fig.4.1 presents the system configuration when BESS is connected to the utility grid. In this system configuration, BESS is connected locally in shunt with the load. BESS compensates active and reactive power requirement of the localized load under certain developed control conditions. Intermittency in DG due to RES is curbed by the Battery Energy Storage System (BESS) i.e. STATCOM with energy storage system. BESS is designed with such capacity that it can support DG of the maximum capacity which is the part of that microgrid.

The main objective of the system configuration is to provide support during intermittency in DG due to RES such that power flowing from the utility grid does not change abruptly. The power flow from the grid must change smoothly during any transition in the DG such that stability of the utility system does not get disturbed. BESS caters to real and reactive power requirement and thus grid side stress is reduced in case there is sudden surge in load demand.

4.3.2.1 Control Algorithm

Here battery energy storage system (BESS) is connected in shunt with the load. It acts as a current controlled source. Due to intermittency in DG due to RES, the real power flow from DG abruptly changes which affects the flow of power from grid side. The battery energy storage system (BESS) abruptly compensates for the change in the real power flow from DG such that power flowing from the grid side does not change abruptly. This compensation from BESS is decreased gradually at the droop rate so that smooth power flow from the grid side takes place to meet the load requirements. This reduces sudden transitions in power flow from the grid side thus ensuring power system stability during intermittency of RES.

Battery energy storage system (BESS) as a current controlled source compensates by delivering/absorbing the real and reactive components of current. DG having RES is a source supplying real power. The control algorithm developed for creating virtual inertia and for compensating the reactive components through BESS is analyzed in dq-frame of reference wherein d- component of current corresponds to real power component and q-component of current corresponds to reactive power component that is being injected through BESS to the system. Fig.4.3 represents the block diagram for generating d-component of reference current (I_{dref}) in the control algorithm for real power compensation through battery energy storage system (BESS).

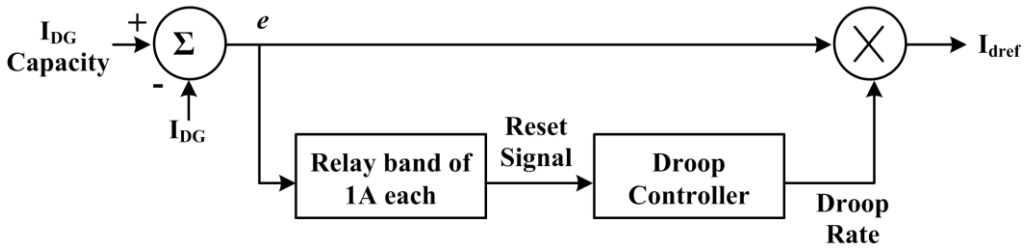

Fig.4.3 Block diagram for developing I_{dref}

DG is designed to work at its maximum capacity. Due to intermittency of RES, the current supplied by DG to the grid fluctuates which is sensed and compared with the current supplied by DG when working at its maximum capacity. The difference between these two current values (e) as depicted in fig.4.4 is passed through a current band having a tolerance of 1A and is then passed through resettable droop reference generator so as to initiate the droop slope at different intermittent values of current supplied by DG. If the difference of the above mentioned currents at any instant of time lies within 1A, then it remains in the same tolerance band such that the resettable droop reference generator does not reset its value and follow the same droop rate corresponding to the difference of current supplied by DG at previous instant of time and the current supplied by DG when operating at maximum capacity.

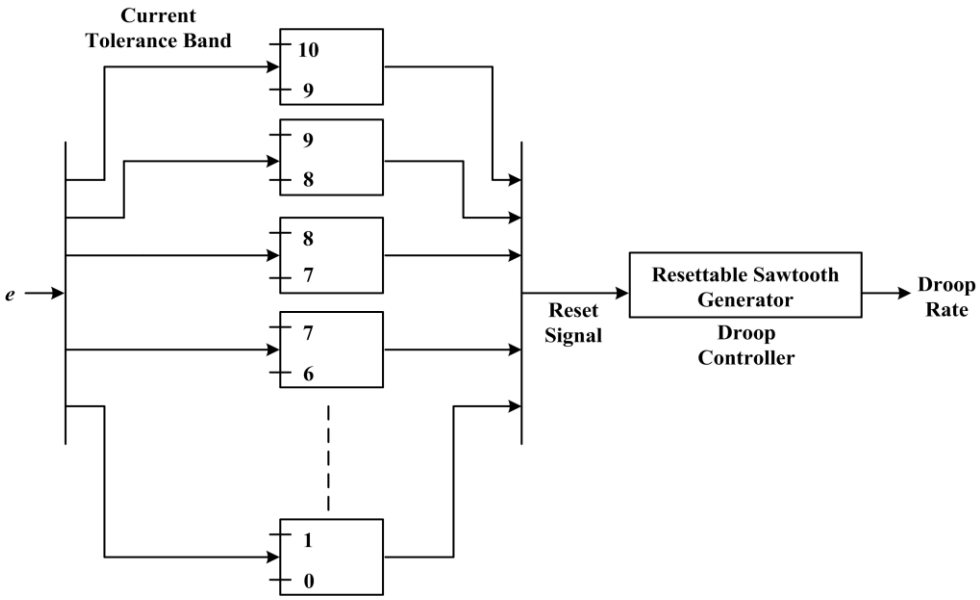

Fig.4.4 Resettable droop controller with current tolerance band

The negative slope ramp pulse generator is activated / triggered when current supplied by DG changes with respect to the current supplied by DG when working at its maximum capacity. Requisite magnitude of ramp pulse having constant negative slope being the difference of the magnitude of the current supplied by DG and the current supplied by DG when operating at the maximum capacity is triggered in case the current supplied by DG decreases abruptly by more than 1A. This in turn provides I_{dref} for real power compensation through BESS. BESS delivers the real power to the load instantly as required by the load.

If the current supplied by DG at an instant of time is more than the current supplied by DG at previous instant of time then positive ramp pulse generator is activated/triggered. In case the current supplied by DG increases abruptly by more than tolerance band of 1A, then positive slope ramp pulse generator is activated/triggered with specific positive droop rate such that BESS absorbs requisite amount of excess real power instantly and delivers this absorbed power to the system at this droop rate such that power flow from the grid does not fall abruptly and follow a smooth transition thus ensuring stable operation of the utility grid.

For voltage regulation at PCC, the voltage at PCC is compared with the standard reference voltage which is passed through PI controller generating current requisite to the reactive current reference. This reactive current reference is summed up with the

reactive current component required for compensating reactive power requirement of the load to generate total reactive component (I_{qref}) which maintains terminal voltage at PCC and simultaneously supply reactive power demanded by the load. Fig.4.5 presents the block diagram for generating q-component of reference current (I_{qref}) in the control algorithm for reactive power compensation through BESS and for regulating terminal voltage at PCC.

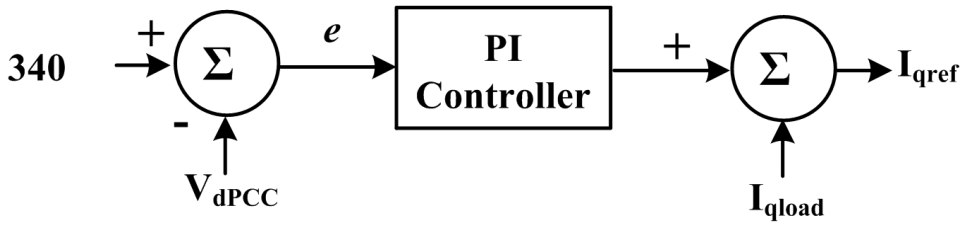

Fig.4.5 Block diagram for developing I_{qref}

4.4 CONCLUSION:

It is evident from the control algorithm that the real component supplied by the BESS is such that it instantaneously compensates for the intermittency of RES at a specific droop rate in order to meet the load requirement and reducing fluctuations as observed in the utility grid. The real component supplied by the BESS varies with a definite droop rate such that real power flow from the grid varies gradually with a definite droop rate. Thus droop control helps in creating virtual inertia in the power inverters which further maintains system stability during intermittent operation of DG. The reactive component supplied by battery energy storage system (BESS) helps in maintaining voltage at PCC.

CHAPTER 5
SIMULATION RESULTS AND DISCUSSIONS

5.1 GENERAL INTRODUCTION

This chapter presents simulation results for the verification of proposed control algorithm to incorporate virtual inertia with the battery energy storage system during intermittent operation of RES based DG. The simulation results presented in this chapter depicts the grid current, power transacted through DG and battery energy storage system (BESS) in a microgrid.

5.2 SIMULATION RESULTS

Based on the control algorithm developed in the previous chapter, the proposed algorithm is simulated in MATLAB simulink. Simulation results for the various cases are presented here:

5.2.1 Case 1: When battery energy storage system (BESS) is not connected to the utility grid

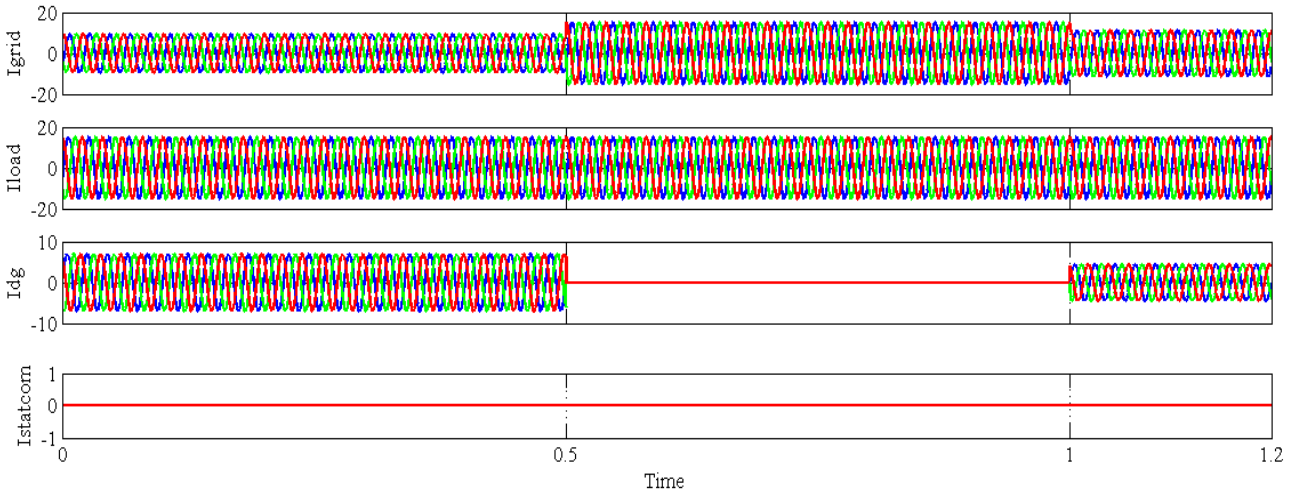

Fig.5.1 Current flow without battery energy storage system (BESS)

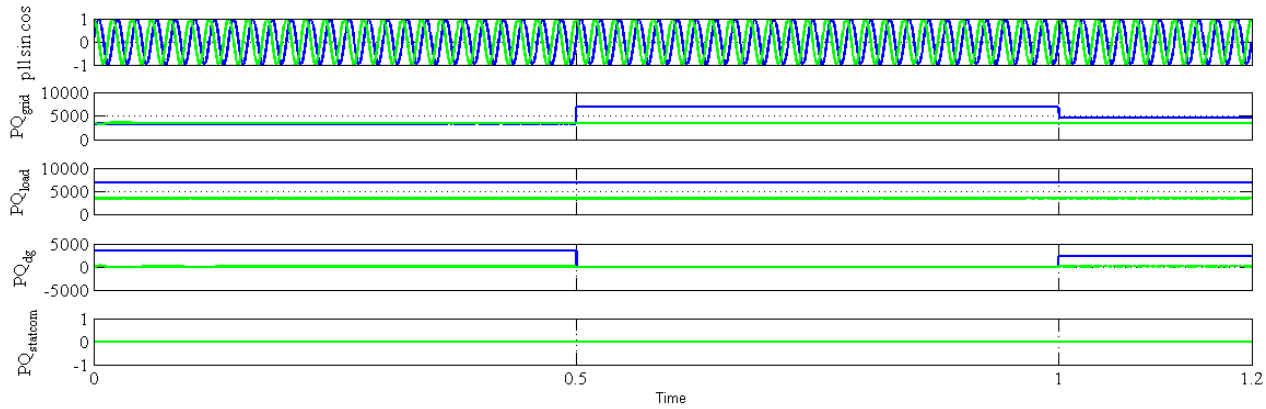

Fig.5.2 Power flow without battery energy storage system (BESS)

Fig 5.1: Represents the current flow in a microgrid when no BESS is connected into system. At time t= 0 sec., DG is supplying current when it is working at its maximum capacity i.e. DG is supplying current of 7A at time t= 0 sec. At time t=0.5 sec, due to intermittency in DG, real power supplied by DG becomes zero. At time t=0.5 sec real power flow from grid to the load suddenly increases in order to cater to the demand on the load side.

At time t=1 sec , DG is again connected to the system utility. This causes localized real power demand satisfaction to the load, thus real power flow from the grid decreases abruptly which is evident in fig.5.1. The real power flow from grid makes a transition at t=1 sec and drops to 5 kW. This abrupt power flow from grid creates instability in the power system. Fig 5.1 represents that the real and reactive power demanded by load is being catered by the grid in the absence of DG. During the operation of DG real power demanded by the load is being shared by DG and the grid.

5.2.2 Case 2: When BESS is connected to utility grid in the presence of R – load.

Fig 5.3:- Represents the power flow in a microgrid in case of R-load when BESS is connected into the system. Load being resistive demands only active power. At time t=0 sec this active power requirement is shared by DG working at its maximum capacity and the utility grid. At time t=0.5 sec as DG stops supplying real power abruptly, this real power demand is compensated instantly by BESS and then real power flow from the grid is increased gradually following the droops with definite

slope till the entire real power demand of the load is catered by the utility grid. At t=1.0 sec, when DG again starts supplying real power to the utility load then BESS absorbs this excess power instantly and starts delivering this power at definite droop rate such that real power flow from the grid drops gradually following the same droop rate till the entire power required by load is supplied by the grid and DG.

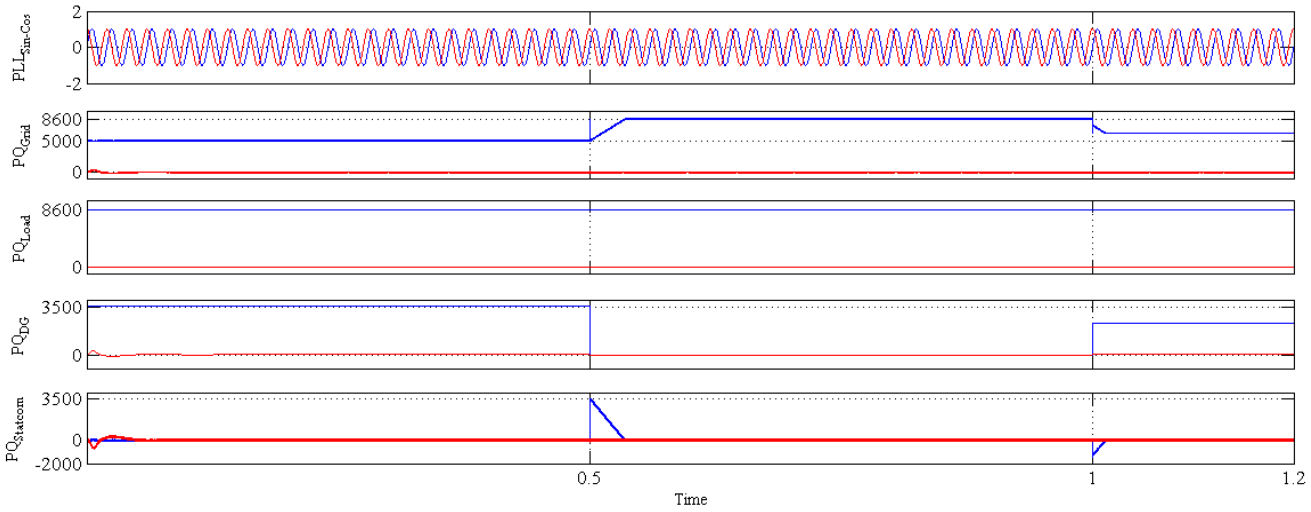

Fig.5.3 Power flow with battery energy storage system (BESS) when connected to R - Load

Only real power compensation takes place through battery energy storage system (BESS). As there is no reactive power requirement of the load, so reactive power compensation is not required to be done through BESS.

5.2.3 Case 3: When BESS is connected to utility grid in the presence of RL– load

Fig 5.4 represents the current flow in a microgrid when battery energy storage system (BESS) is connected to the system. At time t=0 sec. in order to cater real power load demand of 7 kW, grid is supplying is 3.75 kW and DG is supplying 3.25 kW when working at its maximum capacity making real power flow from battery energy storage system (BESS) zero. The reactive power requirement of the load is being catered by BESS locally by supplying 3.5 KVAR to the load so that current flow from the grid is maintained at unity power factor (UPF).

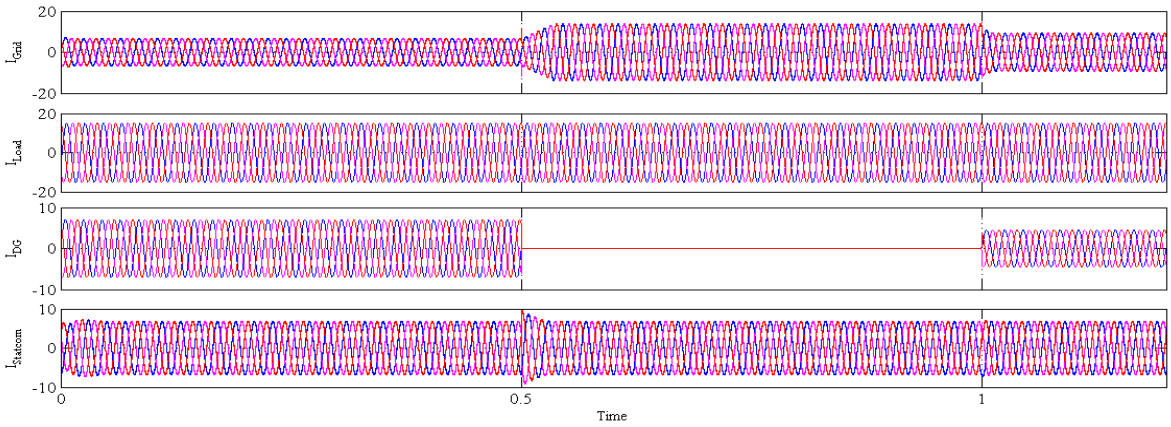

Fig.5.4 Current flow with battery energy storage system (BESS) when connected to RL - Load

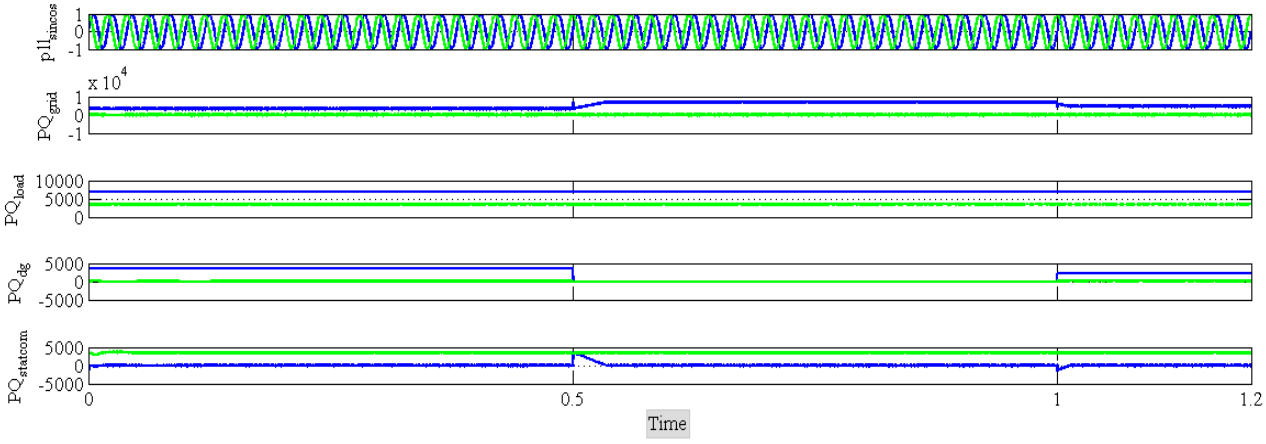

Fig.5.5 Power flow with battery energy storage system (BESS) when connected to RL - Load

Fig.5.5 represents the power flow in the microgrid when battery energy storage system (BESS) is connected to the utility grid supplying real and reactive power to the load.

At time t= 0.5 sec, DG suddenly stops supplying power to the utility because of its intermittent nature. At that instant, real power requirement of the load is catered by BESS so that power flow from the grid to the load does not change abruptly. Further, the real power flow from BESS is decreased gradually with some droop, allowing real power flow from grid to increase gradually. This improves the stability of the utility grid by creating virtual inertia in the power electronic converters interface. The reactive power requirement is catered locally by BESS to maintain unity power factor at the grid side.

At time t=1 sec, DG again comes into operation by supplying real power equivalent to 2.25 kW to the system. This excess power is instant ly absorbed by the BESS to avoid instant decrease in grid current. Thereby, through droop control absorbed BESS current gradually decreases, making grid current drop gradual.

Further, to maintain PCC voltage within permissible limits, the PI controller reduces the variation of this PCC voltage with respect to the reference voltage by supplying the requisite q- component of current.

5.3 CONCLUSION:

From the above analysis and results, it is observed that battery energy storage system (BESS) working as a current controlled source compensates the real and reactive component requirement of the load. Reference droop generator with definite droop slope helps in creating virtual inertia in the power electronic converters which in turn help in maintaining system stability during intermittent operation of RES based DG.

CHAPTER 6
CONCLUSIONS AND FUTURE SCOPE OF WORK

6.1 GENERAL INTRODUCTION

Generation of electricity using RES is gaining importance in recent times due to advent of distributed generation and to reduce the burden on conventional fuels for catering ever increasing load demand. To shape the output voltage and current of these intermittent RES compatible with the grid, power electronics based system comes as a very efficient interface. With greater penetration of RES based DGs having lower inertia into the utility grid, it posed a lot of challenges for power electronic engineers.

6.2 MAIN CONCLUSIONS

This thesis has presented an overview of different aspects related to the control of AC microgrids having penetration of RES based DGs. Droop characteristic based control technique has been presented in this work helps improve the system stability and increase the system reliability.

The main aim of this work is to develop a control algorithm for creating virtual inertia in power electronics converters interfaced with RES. Battery energy storage system (BESS) acting as a current controlled source is connected to the utility grid at the point of common coupling (PCC). A resettable droop controller is developed in the control algorithm which meets its droop amplitude depending on the difference of the magnitude of the current supplied by the DG when working at maximum capacity and at any particular instant time. This algorithm helps in maintaining system stability and allows current to flow from the grid in a gradual manner following the droop slope during intermittent operation of DG in a microgrid. Battery energy storage system

(BESS) also compensates the local reactive power required by the load thus establishing unity power factor at the grid side.

6.3 FUTURE SCOPE OF WORK

The presented control schemes pave the way for variety of additional scope for future research work. Decentralized, centralized and distributed multi – agent control strategies can be designed in order to co-ordinate distributed microgrid ES systems. Precise and accurate droop – control techniques can be designed using adaptive controllers for power sharing between DGs and loads in a microgrid. Further, hardware based realization of the developed control algorithms can be done using the tools and techniques as discussed in this work.

REFERENCES

[1] J.M.Carrasco, L.G.Franquelo, J.T.Bialassiewicz, E.Galvan, R.Portillo, M.M.Prats, J.I.Leon, N.Moreno, Power Electronic Systems for the grid integration of Renewable Energy Sources: a Survey, pp. 1-13

[2] L.H.Hansen, F.Blaabjerg, H.C.Christensen, U.Lindhard, Generators and Power Electronics Technology for Wind Turbines, pp. 2000-2005, ECON'01: the 27th annual conference of the IEEE Industrial Electronics Society.

[3] Tarang Agarwal, Shivank Verma, Issues and challenges of wind energy, pp. 67-72, International Conference on Electrical, Electronics and Optimization Techniques (ICEEOT) – 2016

[4] Varun Kumar, A.S.Pandey, S.K.Sinha, Grid Integration and Power Quality Issues of Wind and Solar Energy System: A Review, pp. 71-80, International Conference on Emerging Trends in Electrical, Electronics and Sustainable Energy Systems (ICETEESES-16)

[5] Hossein Lotfi, Amin Khodaei, AC Versus DC Microgrid Planning, pp. 296-304, IEEE Transactions on Smart Grid, Vol.8, No.1, January 2017

[6] Kalpesh C.Soni, Firdaus F.Belim, Microgrids during grid - connected mode and islanded mode - A Review, NCRRET-2015, IJAERD

[7] A.A.Salam, A.Mohamed, M.A.Hannan, Technical Challenges on Microgrids, pp. 64-69, ARPN Journal of Engineering and Applied Sciences.

[8] D. Semënov, G. Mirzaeva, C. D. Townsend and G. C. Goodwin, "A battery storage control scheme for AC microgrids," 2017 20th International Conference on Electrical Machines and Systems (ICEMS), Sydney, NSW, 2017, pp. 1-6.

[9] G. Cavraro, T. Caldognetto, R. Carli and P. Tenti, "A master/slave control of distributed energy resources in low-voltage microgrids," 2016 European Control Conference (ECC), Aalborg, 2016, pp. 1507-1512.

[10] J. Rocabert, A. Luna, F. Blaabjerg and P. Rodríguez, "Control of Power Converters in AC Microgrids," in IEEE Transactions on Power Electronics, vol. 27, no. 11, pp. 4734-4749, Nov. 2012.

[11] T. Morstyn, B. Hredzak and V. G. Agelidis, "Control Strategies for Microgrids With Distributed Energy Storage Systems: An Overview," in IEEE Transactions on Smart Grid, vol. 9, no. 4, pp. 3652-3666, July 2018.

[12] M. A. Rahman and M. R. Islam, "Different control schemes of entire microgrid: A brief overview," 2016 3rd International Conference on Electrical Engineering and Information Communication Technology (ICEEICT), Dhaka, 2016, pp. 1-6.

[13] X. Wang, J. M. Guerrero, Z. Chen and F. Blaabjerg, "Distributed energy resources in grid interactive AC microgrids," The 2nd International Symposium on Power Electronics for Distributed Generation Systems, Hefei, China, 2010, pp. 806-812.

[14] H. Bevrani, "Microgrid control: A solution for penetration of renewable power," 2017 International Conference on Green Energy and Applications (ICGEA), Singapore, 2017, pp. 46-51.

[15] P. A. Upadhyay and S. K. Joshi, "Models and methods for integrating green power distributed generators in microgrid," 2017 52nd International Universities Power Engineering Conference (UPEC), Heraklion, 2017, pp. 1-6.

[16] Xialing Xu and Xiaoming Zha, "Overview of the researches on distributed generation and microgrid," 2007 International Power Engineering Conference (IPEC 2007), Singapore, 2007, pp. 966-971.

[17] D. Semënov, G. Mirzaeva, C. D. Townsend and G. C. Goodwin, "Recent development in AC microgrid control — A survey," 2017 Australasian Universities Power Engineering Conference (AUPEC), Melbourne, VIC, 2017, pp. 1-6.

[18] D. E. Olivares et al., "Trends in Microgrid Control," in IEEE Transactions on Smart Grid, vol. 5, no. 4, pp. 1905-1919, July 2014.

[19] P. R. Khatri, V. S. Jape, M. Lokhande and B. S. Motling, "Improving power quality by distributed generation," 2005 International Power Engineering Conference, Singapore, 2005, pp. 675-678 Vol. 2.

[20] H. Han, Y. Liu, Y. Sun, M. Su and J. M. Guerrero, "An Improved Droop Control Strategy for Reactive Power Sharing in Islanded Microgrid," in IEEE Transactions on Power Electronics, vol. 30, no. 6, pp. 3133-3141, June 2015.

[21] S. Golestan, M. Joorabian, H. Rastegar, A. Roshan and J. M. Guerrero, "Droop based control of parallel-connected single-phase inverters in D-Q rotating frame," 2009 IEEE International Conference on Industrial Technology, Gippsland, VIC, 2009, pp. 1-6.

[22] R. A. Mastromauro, M. Liserre, A. Dell'Aquila, J. M. Guerrero and J. C. Vasquez, "Droop control of a multifunctional PV inverter," 2008 IEEE International Symposium on Industrial Electronics, Cambridge, 2008, pp. 2396-2400.